Information rates of radiation as a photon gas

Alfonso Martinez*
CWI, Kruislaan 413, 1098 SJ Amsterdam, The Netherlands
(Received 10 August 2007; revised manuscript received 8 October 2007; published 26 March 2008)

The information rates achievable with a photon-gas model of electromagnetic radiation are studied. At any frequency, information rates over the photon-gas model essentially coincide with the Shannon capacity when the signal-to-noise ratio is below a threshold. Only above the threshold does the photon gas incur in a significant loss in information rates; the loss can amount to half of the capacity. The threshold exceeds 40 dB for radio frequencies and vanishes at higher frequencies.

DOI: 10.1103/PhysRevA.77.032116 PACS number(s): 03.65.Yz, 42.50.Ar, 03.67.Hk

I. INTRODUCTION

The addition of quantum effects to Shannon's classical information theory has a rich history, from the pioneering analysis of Gordon [1,2], through significant contributions by Helstrom [3] and Holevo [4,5], up to more recent work by Giovannetti *et al.* [6,7]. A goal shared by these authors has been the derivation of Shannon's expression for the capacity of a wave-form channel with Gaussian noise from quantum-mechanical principles.

In nats (1 nat is $\log_2(e)$, or 1.4427, bits) per Fourier mode, the Shannon capacity C_{Sh} of the complex-valued Gaussian channel is given by the well-known expression [8]

$$C_{\mathrm{Sh}}(E_s,\sigma^2) = \ln(E_s+\sigma^2) - \ln(\sigma^2), \tag{1}$$

where E_s is the average received energy per mode and σ^2 is the corresponding Gaussian noise variance, in turn given by $\sigma^2=N_0$, where N_0 is the one-sided (thermal) noise spectral density.

In one approach, analyzed by Gordon [1,2], information is sent over coherent states and recovered at the receiver by performing a coherent heterodyne measurement. In this case, noise is additive Gaussian with variance $(\varepsilon_n+1)h\nu$, where ε_n is the average number of thermal photons in the corresponding mode of frequency ν; the average energy E_s similarly becomes $E_s=\varepsilon_s h\nu$, ε_s being the average number of signal photons. The capacity with heterodyne detection C_{Het} is given by [1,9]

$$C_{\mathrm{Het}}(\varepsilon_s,\varepsilon_n) = \ln(1+\varepsilon_s+\varepsilon_n) - \ln(1+\varepsilon_n). \tag{2}$$

In the absence of restrictions on the measurement method, one can use the Holevo-Schumacher-Westmoreland (HSW) theorem to compute the largest information rate achievable. When the channel inputs are not entangled and no entangled measurements are allowed one obtains the so-called one-shot capacity. For coherent—i.e., Gaussian—states the corresponding one-shot capacity, which we denote by C_{HSW}, is given by [4–6]

$$C_{\mathrm{HSW}}(\varepsilon_s,\varepsilon_n) = g(\varepsilon_s+\varepsilon_n) - g(\varepsilon_n), \tag{3}$$

where $g(t)$ is the entropy of a Bose-Einstein distribution with mean t, given by $g(t)=(1+t)\ln(1+t)-t\ln t$, with the agreement that $0\ln 0=0$. Using entanglement does not increase the capacity in absence of thermal noise, i.e., for $\varepsilon_n=0$ [6]. For other values of ε_n, entanglement might yield a larger capacity, although this formula is conjectured to be the capacity also in that case [7].

For radio and microwave frequencies $\varepsilon_n \gg 1$ and the noise spectral density satisfies $N_0=\varepsilon_n h\nu \simeq kT_0$, T_0 being the ambient temperature. Moreover, the Shannon capacity C_{Sh} is very close to the capacity with coherent heterodyne detection and to the one-shot, coherent-state capacity, that is

$$C_{\mathrm{Het}}(\varepsilon_s,\varepsilon_n) \simeq C_{\mathrm{HSW}}(\varepsilon_s,\varepsilon_n) \simeq C_{\mathrm{Sh}}(E_s,kT_0). \tag{4}$$

Details can be found in Appendix A. Any of these equations gives thus the largest information rate practically achievable when thermal noise is the limiting factor.

Inspired by recent work on reference frames in information theory [10], where Schumacher is quoted as saying that "restrictions on the resources available for communication yield interesting communication theories," we consider a model of radiation as an ensemble of classical particles, for which quantum interference terms are absent. Rather than adding quantum effects, we examine the effect on the information rates of removing some of the quantum behavior of radiation.

In Sec. II we present a discrete channel model of the radiation field as a photon gas. The key trait of the photon-gas model is that information is sent by modulating the energy of the Fourier modes of the field. Likewise, energy is measured at the receiver. The received signal is the sum of thermal noise, distributed as blackbody radiation at a given temperature and frequency, and a useful signal whose energy distribution is the same as for a coherent state. As with direct detection methods at optical frequencies [9], communication over a photon gas cannot rely on knowledge of the phase of coherent states.

In Sec. III we determine the channel capacity of the photon-gas model and derive the main result of this paper, namely that the information rate of the photon gas essentially coincides with Shannon's capacity, with the capacity of heterodyne detection, and with the one-shot coherent-state capacity in Eq. (4) above, provided that the signal-to-noise ratio lies below a threshold; above the threshold, up to half of the capacity may be lost. At 290 K and for a frequency ν (in Hertz), this threshold is approximately given by $\frac{6\times 10^{12}}{\nu}$

*alfonso.martinez@ieee.org

and is thus large for radio and microwave frequencies. Moreover, in the "classical" limit where energy is continuous the capacity of the photon gas coincides with Shannon's capacity C_{Sh}.

II. MODEL OF RADIATION AS A PHOTON GAS

In this section, we describe a model of the radiation field as a photon gas. The model is obtained from the usual quantum analysis by assuming that radiation behaves as classical particles, with no quantum interference effects. Even though this postulate does not arise naturally from electromagnetic theory, the resulting model is well-defined and leads to useful insights on the amount of information which can be sent by using electromagnetic radiation.

Consider one polarization of the electromagnetic field at an aperture, which we denote by $\tilde{y}(t)$, a complex-valued function representing the positive-frequency components of the received field. Throughout the paper we use a tilde to indicate that the function represents a field amplitude. As is well-known, the field $\tilde{y}(t)$ admits a Fourier decomposition onto frequencies of the form $\nu_c+\frac{m}{T}$, lying in a band of width W around a reference frequency ν_c; here T is the duration of the observation interval. The mth basis function is then given by $\theta_m(t)=\frac{1}{\sqrt{T}}e^{-i2\pi(\nu_c+m/T)t}$. Further, let the field $\tilde{y}(t)$ represent the superposition of a useful signal $\tilde{x}(t)$ and of additive Gaussian noise $\tilde{z}(t)$, respectively given by

$$\tilde{x}(t)=\sum_m \tilde{x}_m\theta_m(t), \quad \tilde{z}(t)=\sum_m \tilde{z}_m\theta_m(t); \tag{5}$$

here $\tilde{x}_m$ is the field amplitude for the useful signal at mode m, set at the transmitter (except for a propagation loss and a phase rotation), and $\tilde{z}_m$ are samples of Gaussian noise, e.g., thermal radiation at a given temperature T_0 and frequency ν_m.

In a quantum description, the fields $\tilde{y}(t)$, $\tilde{x}(t)$, and $\tilde{z}(t)$ are replaced by operators representing the positive-frequency components of the vector potential; each Fourier mode represents then one degree of freedom of the electromagnetic field. In particular, the received field $\tilde{y}(t)$ is represented by a set of annihilation operators $\hat{y}_m$, one for each mode. The superposition of signal and noise is then represented by a completely positive, trace-preserving map [11], which combines the annihilation operators of the electromagnetic field for the useful signal, denoted by $\hat{x}_m$, and additive noise, $\hat{z}_m$; this map guarantees that the output operators satisfy the bosonic commutation rules. The superposition is given by [12]

$$\hat{y}_m=\sqrt{\eta}e^{i\phi_x}\hat{x}_m+\sqrt{1-\eta}e^{i\phi_z}\hat{z}_m. \tag{6}$$

The channel maps the two input annihilation operators onto two outputs, the additional output being

$$-\sqrt{1-\eta}e^{-i\phi_z}\hat{x}_m+\sqrt{\eta}e^{-i\phi_x}\hat{z}_m. \tag{7}$$

This guarantees the conservation of energy while the fields are added [12]. We assume that η, ϕ_z, and ϕ_x are independent of the mode index. The model includes thus the channel propagation loss η and the phase uncertainty.

When the phases ϕ_z and ϕ_x are known at the receiver, a coherent detection receiver acts on the annihilation operator $\hat{y}_m$ [9] and measures a quantity $\tilde{y}'_m=\sqrt{\eta}\tilde{x}_m+\tilde{z}'_m$, except for an irrelevant phase. Here $\tilde{x}_m$ is set at the transmitter and $\tilde{z}'_m$ is a Gaussian random variable of variance $[(1-\eta)\varepsilon_n+1]h\nu$, where ε_n is the average number of thermal photons.

As an alternative, a direct detection receiver measures the number operator $\hat{y}^\dagger_m\hat{y}_m$ for the mth received temporal mode, namely

$$\hat{y}^\dagger_m\hat{y}_m=\eta\hat{x}^\dagger_m\hat{x}_m+(1-\eta)\hat{z}^\dagger_m\hat{z}_m+[\sqrt{\eta(1-\eta)}e^{-i(\phi_x-\phi_z)}\hat{x}^\dagger_m\hat{z}_m+\mathrm{H.c.}]. \tag{8}$$

Measurement of the number operator $\hat{y}^\dagger_m\hat{y}_m$ generates an output which can be modeled as a random variable y_m distributed according to a Laguerre distribution with parameters $\eta\frac{|\tilde{x}_m|^2}{h\nu}$ and $(1-\eta)\varepsilon_n$ [13]. In the approximation that the energy is continuous, y_m follows a noncentral chi-square distribution.

Our photon-gas model is obtained by postulating the removal of the interference term $\hat{x}^\dagger_m\hat{z}_m$ (and its Hermitian conjugate), whose form is that of a quantum interference term, while maintaining the rest of the standard model. Radiation is thus represented as an ensemble of classical particles. The measurement y_m is now given by

$$y_m=\eta\hat{x}^\dagger_m\hat{x}_m+(1-\eta)\hat{z}^\dagger_m\hat{z}_m, \tag{9}$$

namely the sum of the energies of signal and noise.

The signal component $\eta\hat{x}^\dagger_m\hat{x}_m$ is modeled as a Poisson random variable, of mean $\eta\frac{|\tilde{x}_m|^2}{h\nu}$, where $\tilde{x}_m$ is the field value set at the transmitter. As for the additive noise component $(1-\eta)\hat{z}^\dagger_m\hat{z}_m$, it has a Bose-Einstein distribution [9] of mean $(1-\eta)\varepsilon_n$, where ε_n is the average number of thermal photons at the corresponding frequency and temperature. Since $\eta\leqslant 1$, the distributions of signal and noise components remain Poisson and Bose-Einstein, with the respective means reduced by the corresponding factor, η or $1-\eta$ [13].

One can think of this model as a photon gas, where the receiver counts the number of photons in each Fourier mode. For a continuous-energy approximation, the noise energy has an exponential density, which is both the limiting form of a Bose-Einstein distribution and the density of the squared amplitude of complex Gaussian noise [13]. In turn, the Poisson distribution approaches a delta function at the received energy $\eta|\tilde{x}_m|^2$.

III. INFORMATION RATES

In the previous section we introduced two representations of radiation as a photon gas: a model where the energy of each Fourier mode is discrete and an exponential noise model for which the energy is continuous. In both cases, we have a channel model of the form

$$y_m=s_m(x_m)+z_m, \quad m=1,\ldots,n, \tag{10}$$

where y_m is a measurement on the mth Fourier mode, x_m is the mth signal component, a non-negative real number set at the transmitter, s_m the useful signal at the output, and z_m is

the mth sample of additive noise. By construction, the signal s_m and the noise z_m are independent of each other; the noise components z_m are also independent for different values of m.

The specifics of each of the two models are as follows.

(1) For discrete energy, y_m, s_m, and z_m are numbers of photons, each of energy $h\nu$. The signal component s_m has a Poisson distribution with mean ηx_m, where η is a propagation loss between transmitter and receiver. In field notation, $x_m = \frac{|\tilde{x}_m|^2}{h\nu}$. The noise component z_m has a Bose-Einstein distribution. One example is thermal radiation at temperature T_0 attenuated by a factor $(1-\eta)$, with mean $\varepsilon_n = (1-\eta)(e^{h\nu/kT_0}-1)^{-1}$. At near-visible and visible wavelengths, where scattered sunlight is the dominant noise source, the temperature T_0 can be an effective temperature, with typical values of the order of some thousands of Kelvin.

(2) For continuous energy, that is $\varepsilon_s \gg 1$ and $\varepsilon_n \gg 1$, then y_m, $s_m = \eta x_m$ and z_m are non-negative real numbers, the energy in the mth mode. The density of the random variable signal energy approaches a delta function, since $p_{S|X}(s_m h\nu | x_m h\nu) \to \delta((s_m - x_m)h\nu)$. For thermal noise, z_m are samples of exponential noise with mean $E_n = (1-\eta)kT_0$.

In all cases, we impose a constraint on the average received signal energy E_s; E_s is related to the average transmitted energy E_t as $E_s = \eta E_t$. We denote by ε_s the average number of received signal photons. We consider only narrowband channels, for which the frequency ν is assumed constant for all modes.

The largest information rate (measured in nats per Fourier mode) that can be sent over a channel with output conditional density $p_{Y|X}(y|x)$ is the channel capacity C [8], given by

$$C = \sup_{p_X(x)} I(X;Y), \tag{11}$$

where the maximization is over all input densities $p_X(x)$ satisfying the energy constraint, and $I(X;Y)$ is the mutual information between channel input and output. For continuous output the mutual information is given by

$$I(X;Y) = \int\int p_X(x) p_{Y|X}(y|x) \ln \frac{p_{Y|X}(y|x)}{p_Y(y)} dy dx, \tag{12}$$

where $p_Y(y) = \int p_X(x) p_{Y|X}(y|x) dx$. For discrete output, the integrals over y should be replaced by sums.

Under the approximation that the energy is continuous, we previously saw that Poisson noise vanishes and the Bose-Einstein distribution turns into an exponential density. The capacity C_{AEN} of a channel with additive exponential noise was studied by Verdú [14]. Applied to our channel model, we obtain the somewhat surprising

$$C_{\mathrm{AEN}}(E_s, E_n) = \ln(E_s + E_n) - \ln(E_n), \tag{13}$$

as in the classical limit with Gaussian noise. Shannon's capacity is thus achieved even though the quadrature components of the field are not explicitly used. In the next section, we determine the capacity of the photon gas and compare its value with the capacity of several quantum models.

IV. CAPACITY OF THE PHOTON GAS

In the photon-gas model, two sources of noise are present at the output: Poisson noise, arising from the signal itself, and additive noise. Distinct behavior is to be expected depending on which noise prevails.

In a first approximation, the behavior is determined by the noise variance. The additive noise variance is given by $\varepsilon_n(1+\varepsilon_n)$ (it follows a Bose-Einstein distribution), whereas the average signal variance is ε_s (as befits a Poisson random variable) [13]. For $\varepsilon_n \gg 1$, a region of practical importance, the variances coincide if $\varepsilon_s = \varepsilon_n^2$. We denote this value of ε_s by ε_s^*. For lower values of ε_s, additive noise prevails; at higher signal energies, Poisson noise dominates. In the next section we examine how this change of behavior translates into the achievable information rates. Then, we discuss in some detail the behavior of the photon gas for radio and microwave frequencies and for optical frequencies.

A. Upper and lower bounds to the capacity

As proved in Appendix B, the capacity $C(\varepsilon_s, \varepsilon_n)$ of the photon-gas model is upper bounded by C_{Upp}, as

$$C_{\mathrm{Upp}}(\varepsilon_s, \varepsilon_n) = \min[C_{\mathrm{G}}(\varepsilon_s, \varepsilon_n), C_{\mathrm{P}}(\varepsilon_s)], \tag{14}$$

where C_{G} and C_{P} are, respectively, given by

$$C_{\mathrm{G}}(\varepsilon_s, \varepsilon_n) = g(\varepsilon_s + \varepsilon_n) - g(\varepsilon_n) = C_{\mathrm{HSW}},$$

$$C_{\mathrm{P}}(\varepsilon_s) = \ln\left[\left(1 + \frac{\sqrt{2e}-1}{\sqrt{1+2\varepsilon_s}}\right)\frac{\left(\varepsilon_s + \frac{1}{2}\right)^{\varepsilon_s + 1/2}}{\sqrt{e}\,\varepsilon_s^{\varepsilon_s}}\right]. \tag{15}$$

Here $g(t)$ is the entropy of a Bose-Einstein distribution with mean t. In particular, the one-shot capacity of the quantum channel with coherent states, C_{HSW}, is an upper bound to the capacity of the photon-gas model. The second bound C_{P} is the capacity of a discrete-time Poisson channel, for which $\varepsilon_n = 0$.

Both functions C_{G} and C_{P} are monotonically increasing functions of ε_s. For sufficiently high signal energy levels, the bound C_{P} prevails over C_{G}. Both bounds thus have a crossing point, whose position we next determine for high signal and noise energy levels, i.e., $\varepsilon_n \gg 1$ and $\varepsilon_s \gg \varepsilon_n$. Using the asymptotic forms of the upper bounds from Appendix A, we have

$$C_{\mathrm{G}}(\varepsilon_s^*, \varepsilon_n) \simeq \ln\left(\frac{\varepsilon_s^*}{\varepsilon_n}\right) \simeq \frac{1}{2}\ln(\varepsilon_s^*) \simeq C_{\mathrm{P}}(\varepsilon_s^*), \tag{16}$$

and we obtain again the expression $\varepsilon_s^* = \varepsilon_n^2$, previously derived by reasoning in terms of noise variance.

In this classical limit, in the sense of large photon counts, we can use the classical formula of the average signal-to-noise ratio (SNR), $\mathrm{SNR} = E_s/E_n$. Further, we assume that $\eta \ll 1$, so that $E_n = h\nu\varepsilon_n$ is approximately given by kT_0 as $\varepsilon_n \simeq (kT_0)/(h\nu)$. For thermal noise we can then define a threshold signal-to-noise ratio (SNR*) as

$$\mathrm{SNR}^* = \frac{E_s}{E_n} \simeq \frac{\varepsilon_s^* h\nu}{kT_0} \simeq \frac{\varepsilon_n^2 h\nu}{kT_0} \simeq \frac{kT_0}{h\nu} \simeq \frac{6\times 10^{12}}{\nu}, \quad (17)$$

where in the last equation we took $T_0=290$ K. In decibels, $\mathrm{SNR}^*(\mathrm{dB}) \simeq 37.8 - 10\log_{10}\nu$ (ν in GHz). This quantitative analysis is valid for radio and microwave frequencies. Similar considerations will be presented later for optical frequencies.

The threshold in the upper bounds is mirrored by a similar behavior for lower bounds. First, we numerically compute a numerical lower bound C_{Low}, namely the largest of the mutual informations achieved by one of the following two input densities (for $x \geqslant 0$):

$$p_X(x) = \frac{\varepsilon_s}{(\varepsilon_s+\varepsilon_n)^2} e^{-x/(\varepsilon_s+\varepsilon_n)} + \frac{\varepsilon_n}{\varepsilon_s+\varepsilon_s}\delta(x), \quad (18)$$

$$p_X(x) = \frac{(1+2\varepsilon_s)^{1/2}}{\sqrt{2e}-1+(1+2\varepsilon_s)^{1/2}} \frac{1}{\sqrt{2\pi x\varepsilon_s}} e^{-x/2\varepsilon_s} + \frac{\sqrt{2e}-1}{\sqrt{2e}-1+(1+2\varepsilon_s)^{1/2}}\delta(x). \quad (19)$$

The first density is also the optimum input distribution for the additive exponential noise channel, as determined by Verdú [14]. In Appendix C we prove that the channel output Y follows a Bose-Einstein output distribution with mean $\varepsilon_s+\varepsilon_n$ when the input X is distributed according to this density and additive Bose-Einstein noise Z is added. As for the second density, it was used in [15] to derive an upper bound to capacity of a discrete-time Poisson channel, specifically the formula for C_{P}.

In addition, we derive in Appendix C a closed-form lower bound to the capacity by using the density in Eq. (18). Its value is

$$C_{\mathrm{Exp}} = g(\varepsilon_s+\varepsilon_n) - \frac{\varepsilon_n}{\varepsilon_s+\varepsilon_n} g(\varepsilon_n) - \frac{\varepsilon_s}{2(\varepsilon_s+\varepsilon_n)} \times \left[\ln 2\pi e + \ln\left[\varepsilon_n(1+\varepsilon_n) + \frac{1}{12} \right] \times e^{\varepsilon_n(1+\varepsilon_n)+1/12/\varepsilon_s+\varepsilon_n} \Gamma\left(0, \frac{\varepsilon_n(1+\varepsilon_n)+\frac{1}{12}}{\varepsilon_s+\varepsilon_n} \right) \right], \quad (20)$$

where $\Gamma(0,t)$ is given by $\Gamma(0,t)=\int_t^\infty u^{-1}e^{-u}du$.

B. Capacity for radio and microwave frequencies

The threshold can be seen in Fig. 1, which depicts the upper (C_{G} and C_{P}) and lower bounds (C_{Low}) to the capacity (in bits) as a function of the input number of quanta ε_s and for several values of ε_n, 1, 10^3, and 10^6 thermal photons. Theloss in the photon-gas model is negligible when, say, $\varepsilon_s < \frac{1}{10}\varepsilon_s^*$. On the other hand, above the energy level $10\varepsilon_s^*$, the upper bound C_{P} becomes dominant. As we will determine later, compared to Shannon's capacity for coherent models, half of the achievable information rate is eventually lost at large values of the signal energy. Since the upper and lower bounds are very close, we conclude that the capacity is closely given by the upper bound in Eq. (14). Around the threshold a small gap of about 1 bit between the upper and lower bounds is visible.

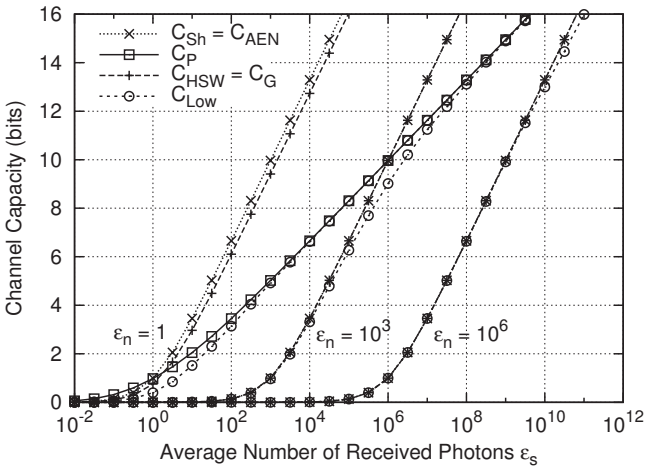

FIG. 1. Bounds to the capacity for several values of ε_n.

As proved in Appendix A, for finite values of ε_s, the upper bound C_{G} (and thus C_{HSW}) satisfies

$$\ln\left(1+\frac{\varepsilon_s}{\varepsilon_n+1}\right) < C_{\mathrm{G}}(\varepsilon_s,\varepsilon_n) < \ln\left(1+\frac{\varepsilon_s}{\varepsilon_n}\right) \quad (21)$$

and thus lies between Shannon's classical capacity and the capacity of heterodyne detection. Moreover, the gap between the various capacities vanishes as ε_s and ε_n go to infinity. Shannon's classical capacity, Eq. (1), is also depicted in Fig. 1. For $\varepsilon_n=10^3$ and 10^6, C_{Sh} is indeed indistinguishable from C_{G}. As $\varepsilon_n \to \infty$ [see Eq. (A5) in Appendix A], the bound C_{G} and the capacity itself approach that of a continuous-energy model, namely C_{AEN}.

At radio and microwave frequencies and for not too large signal-to-noise ratios, there are thus four models which give essentially the same channel capacity. However, for $\varepsilon_n=1$, Shannon's capacity exceeds the result derived from quantum theory by an amount of about 0.56 bits, as we find in Appendix A. We should note here that this low value of ε_n is beyond the classical context where Shannon derived his capacity formula. In general, for low values of ε_n the capacity is more closely given by C_{P}, the capacity of a discrete-time Poisson channel, which we consider in more detail in the following section. For these values of ε_n, the classical signal-to-noise ratio $E_s/E_n=\varepsilon_s/\varepsilon_n$ is not well-defined. As for larger ε_n, a threshold ε_s^* exists such that below it the capacity is closely given by C_{G}; its value corresponds, however, to very low channel capacities.

Figure 2 depicts the information rate loss between the conjectured quantum channel capacity C_{HSW} and our upper and lower bounds. The gap is rather small for energies sufficiently below the threshold and progressively approaches half of the capacity as the input energy grows. For C_{Exp} the

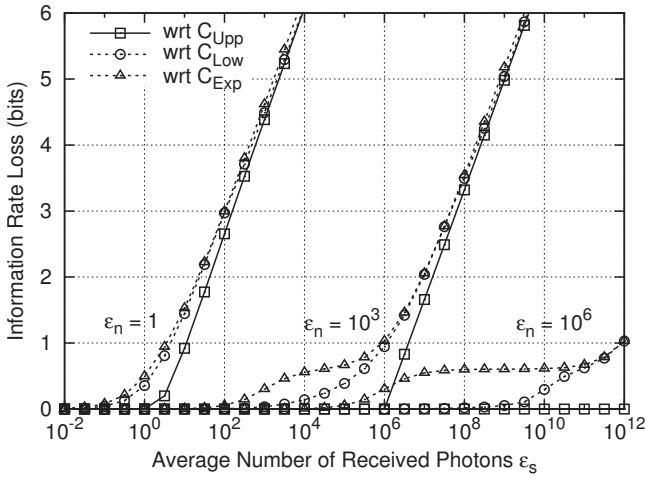

FIG. 2. Bounds to the capacity for several values of ε_n.

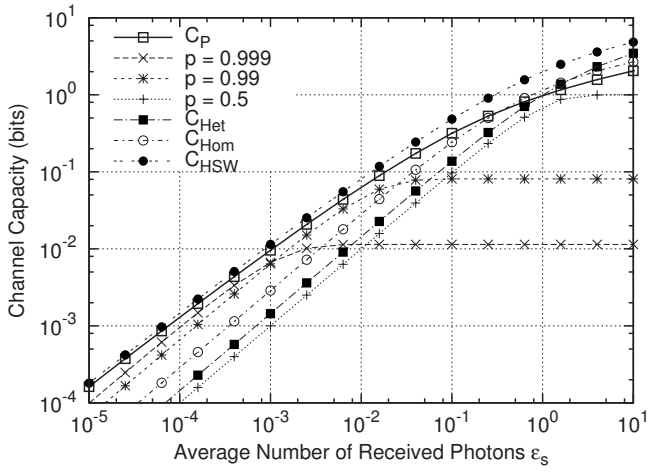

FIG. 3. Discrete-time Poisson channel capacity for flash signaling.

looseness at low ε_s is due to the pessimistic estimate of the conditional output entropy $H(Y|X)$ (details are given in Appendix C), which is smaller than the Gaussian approximation we have used. At high ε_s the tiny gap between C_{Exp} and C_{P} is caused by the nonoptimal input distribution; a closed-form expression derived from Eq. (19) would likely close this gap. The capacity of the photon gas essentially coincides with that of the coherent-state models, even though the phase of the coherent state is not used to transmit information.

A further connection, worthwhile mentioning, can be made with noncoherent communications in Gaussian channels [16], where one of the two signal quadratures is not used, and a change in slope of the capacity function from ln SNR to $\frac{1}{2}$ ln SNR (for high SNR) occurs. A similar limitation arises in phase-noise limited channels [17]. As the threshold SNR* is close to the point where existing digital communication systems using electromagnetic radiation suffer from the effects of phase noise, it would be interesting to verify which of the models, coherent detection or the photon gas, defines most accurately the effective channel capacity. Even though the cost in information rates of the resources spent (e.g., pilots, phase-locked loops) in acquiring and maintaining the phase coherence between transmitter and receiver is small for radio and microwave frequencies, its precise effect on the information rates is difficult to account for and might significantly reduce the capacity for higher frequencies.

C. Capacity for optical frequencies

We next consider optical frequencies, for which ε_n is very small. Thermal noise is negligible and the usual level of ambient light noise will lead to small values of ε_n at the receiver. If the signal level is very low, information transmission is limited by this additive noise component and we fall back onto the case previously considered. As depicted in Fig. 1, very low capacities are achievable. On the other hand, if the signal level is large enough, the dominant noise source is the Poisson noise.

Optical heterodyne coherent detection is close to optimal for large signal energies, in the sense that almost 100% of the classical capacity C_{HSW} can be achieved. More precisely, as we determine in Appendix A, the absolute difference between the two capacities quickly approaches 1.44 bits, which becomes negligible if the capacity is large enough.

Moreover, the capacity with optical direct detection, which corresponds to that of the photon gas, is upper bounded by C_{P}, which asymptotically grows as $\frac{1}{2}\ln \varepsilon_s$, and lower bounded by the mutual information achieved by the density in Eq. (19), or by C_{Exp}, the closed-form expression in Eq. (20). In either case, the capacity of direct detection and therefore that of the photon gas is lower by about a factor $\frac{1}{2}$ than the capacity of the coherent-state models.

At low values of the signal energy, as discussed by Gordon [1], the capacity of homodyne coherent detection, C_{Hom}, exceeds that of heterodyne detection by a factor of 2. This follows from the formula for C_{Hom} [1],

$$C_{\mathrm{Hom}}(\varepsilon_s,\varepsilon_n)=\frac{1}{2}\ln\left(1+\frac{4\varepsilon_s}{2\varepsilon_n+1}\right). \tag{22}$$

Further, binary flash signaling, where one symbol is placed at 0 with probability p and another at $1/(1-p)$ with probability $(1-p)$, achieves a higher mutual information [1]. This is verified in Fig. 3, which depicts the capacity as a function of ε_s of flash signaling for several values of p, together with the capacities for coherent detection and the conjectured quantum capacity C_{HSW}. The envelope of the capacities with flash signaling is close to the upper bound C_{P}, which again proves a good estimate of the capacity of the photon gas.

V. CONCLUSIONS

In this paper, we have studied the channel capacity of a photon-gas model of electromagnetic radiation, whereby radiation is represented by an ensemble of photons—or classical particles—distributed over a set of Fourier modes. We have seen that the photon-gas model need not incur in a significant information rate loss even though the quadrature components of the field are not used separately. In particular, at radio and microwave frequencies, the one-shot capacity of

the quantum channel with coherent states, the capacity with heterodyne coherent detection, and the capacity of the photon gas all essentially coincide with Shannon's formula.

Equivalently, the entropy of the received signal is determined by that of thermal radiation if the signal energy is below a threshold. Below this threshold, the photon-gas model incurs in no information loss; above it, up to half of the channel capacity is lost. The capacity of the photon-gas model thus deviates from that of coherent detection at sufficiently high signal-to-noise ratios.

For a temperature of 290 K, this threshold signal-to-noise ratio is $\frac{6\times10^{12}}{\nu}$, well above the operation of most existing communication systems at microwave frequencies. Above the threshold, such as for higher frequencies, the entropy is determined by the noise in the signal itself, a form of shot noise or Poisson noise.

An open problem is to build a practical communication system whose capacity, including the cost of acquiring and keeping phase synchronization, exceeds the capacity of the photon-gas model and approaches that of the coherent-state model. Previous studies of direct detection [16] showed a non-negligible capacity penalty compared to alternative coherent-state methods. We relate this discrepancy to a different way of accounting for the energy of a mixture of thermal and coherent radiation. In these studies the receiver does not purely detect the sum of the signal and noise energies, but an interference (cross-)term between signal and noise is present. This term has mean zero but nonzero variance; this variance is the source of the penalty in information rate. In our model, this quantum interference term is made to vanish.

Finally, we mention that the photon-gas model is somewhat close to a representation of classical matter as a set of particles. The results presented in this paper may thus be of help in exploring the quantum-classical border for radiation [18].

ACKNOWLEDGMENTS

I wish to thank the anonymous reviewer for his significant contribution to enhancing the content and presentation of the paper. This work was funded by the Freeband Impulse programme of the Ministry of Economic Affairs of the Netherlands and was carried out at the Department of Electrical Engineering of the Technische Universiteit Eindhoven, in Eindhoven, The Netherlands.

APPENDIX A: BOUND ESTIMATES

First, we prove the strict inequality

$$\ln(\varepsilon_s+\varepsilon_n)-\ln\varepsilon_n > C_{\mathrm{G}}(\varepsilon_s,\varepsilon_n) \tag{A1}$$

for all values of $\varepsilon_s>0$, $\varepsilon_n\geqslant 0$. Using the definition of C_{G}, we rewrite this expression as

$$(1+\varepsilon_s+\varepsilon_n)\ln\frac{\varepsilon_s+\varepsilon_n}{1+\varepsilon_s+\varepsilon_n} > (1+\varepsilon_n)\ln\frac{\varepsilon_n}{1+\varepsilon_n}. \tag{A2}$$

This is equivalent to proving that the function $f(t)=(1+t)\ln\frac{t}{1+t}$ is monotonically increasing for $t>0$. It is indeed so since its first derivative $f'(t)$ is

$$f'(t)=\frac{1}{t}-\ln\left(1+\frac{1}{t}\right), \tag{A3}$$

which is positive since $\ln(1+t')<t'$ for positive t'.

We next estimate the gap between the two sides of Eq. (A1) for large ε_s. The gap is given by

$$(\varepsilon_n+1)\ln\frac{\varepsilon_n+1}{\varepsilon_n}-(\varepsilon_s+\varepsilon_n+1)\ln\frac{\varepsilon_s+\varepsilon_n+1}{\varepsilon_s+\varepsilon_n}. \tag{A4}$$

For large ε_s, using that $\ln(1+x)\simeq x$, we get (in bits)

$$(\varepsilon_n+1)\log_2\frac{\varepsilon_n+1}{\varepsilon_n}-\log_2(e). \tag{A5}$$

As $\varepsilon_n\to\infty$, it tends to zero; but it is finite for small ε_n.

We now move on to prove

$$C_{\mathrm{G}}(\varepsilon_s,\varepsilon_n) > \ln(\varepsilon_s+\varepsilon_n+1)-\ln(\varepsilon_n+1). \tag{A6}$$

From the definition of C_{G}, and after canceling common terms, we rewrite the condition as

$$(\varepsilon_s+\varepsilon_n)\ln\frac{1+\varepsilon_s+\varepsilon_n}{\varepsilon_s+\varepsilon_n} > \varepsilon_n\ln\frac{1+\varepsilon_n}{\varepsilon_n}. \tag{A7}$$

This equation is true because the function $f(t)=t\ln(1+\frac{1}{t})$ is monotonically increasing for $t>0$, since it monotonically approaches the number e from below. We can estimate the gap between the two sides of Eq. (A6) for large ε_s. The gap is given by

$$(\varepsilon_s+\varepsilon_n)\ln\frac{1+\varepsilon_s+\varepsilon_n}{\varepsilon_s+\varepsilon_n}-\varepsilon_n\ln\frac{1+\varepsilon_n}{\varepsilon_n}. \tag{A8}$$

For large ε_s, using that $\ln(1+x)\simeq x$, we get

$$\log_2(e)-\varepsilon_n\log_2\frac{\varepsilon_n+1}{\varepsilon_n}. \tag{A9}$$

As $\varepsilon_n\to\infty$, it tends to zero; but it is finite for small ε_n. In particular, the gap between optical heterodyne coherent detection and the classical capacity of the quantum channel approaches $\log_2(e)$ for $\varepsilon_n\to 0$.

APPENDIX B: UPPER BOUNDS

For any input $p_X(x)$ the mutual information satisfies

$$I(X;Y)=H(Y)-H(Y|X) \tag{B1}$$

$$\leqslant g(\varepsilon_s+\varepsilon_n)-H(S(X)+Z|X) \tag{B2}$$

as the Bose-Einstein distribution has the highest entropy under the given constraints [8]. Then,

$$H(S(X)+Z|X)\geqslant H(S(X)+Z|X,S) \tag{B3}$$

$$=H(Z|X)=H(Z) \tag{B4}$$

because conditioning reduces entropy (Chap. 2 of [8]) and Z and X are independent. Therefore

$$I(X;Y)\leqslant g(\varepsilon_s+\varepsilon_n)-g(\varepsilon_n). \tag{B5}$$

As this holds for all inputs the upper bound C_{G} follows.

The variables X, $S(X)$, and $Y(S)$ form a Markov chain in this order, $X \to S(X) \to Y = S(X) + Z$, so that an application of the data processing inequality [8] yields

$$I(X;Y) \leqslant I(X;S(X)), \tag{B6}$$

that is the mutual information achievable in the discrete-time Poisson channel; a good upper bound to the capacity of the latter was given in [15].

APPENDIX C: LOWER BOUND

Our lower bound is derived from the mutual information achievable by a specific input with density in Eq. (18). The channel output induced by this input has a Bose-Einstein distribution and thus achieves the largest entropy. The characteristic function $E[e^{iuY}]$ is given by

$$\frac{1}{1+(\varepsilon_s+\varepsilon_n)(1-e^{iu})}. \tag{C1}$$

As the channel output Y is the sum of two independent random variables, its characteristic function (cf) is the product of the corresponding cf's, namely

$$\frac{1}{1+\varepsilon_n(1-e^{iu})}\int_0^\infty p_X(x)e^{-x(1-e^{iu})}dx \tag{C2}$$

$$= \frac{1}{1+\varepsilon_n(1-e^{iu})}\int_0^\infty \frac{\varepsilon_s e^{-x(1/(\varepsilon_s+\varepsilon_n)+(1-e^{iu}))}}{(\varepsilon_s+\varepsilon_n)^2}dx + \frac{\varepsilon_n}{\varepsilon_s+\varepsilon_n}\frac{1}{1+\varepsilon_n(1-e^{iu})} \tag{C3}$$

$$= \frac{1}{1+\varepsilon_n(1-e^{iu})}\frac{\varepsilon_s}{\varepsilon_s+\varepsilon_n}\frac{1}{1+(\varepsilon_s+\varepsilon_n)(1-e^{iu})} + \frac{\varepsilon_n}{\varepsilon_s+\varepsilon_n}\frac{1}{1+\varepsilon_n(1-e^{iu})}, \tag{C4}$$

which, after grouping and canceling some terms, is Eq. (C1). As a particular case we recover the exponential input, which maximizes the output entropy of a discrete-time Poisson channel [1].

By construction, the output is Bose-Einstein with mean $\varepsilon_s+\varepsilon_n$ and the output entropy $H(Y)$ is therefore given by $H(Y)=g(\varepsilon_s+\varepsilon_n)$. We compute the mutual information with this input as $H(Y)-H(Y|X)$.

We estimate the conditional entropy as

$$H(Y|X) = \int_0^\infty H(Y|x)p_X(x)dx. \tag{C5}$$

We obtain a term $\frac{\varepsilon_n}{\varepsilon_s+\varepsilon_n}H(Y|x=0)$, which can be computed as $H(Y|x=0)=g(\varepsilon_n)$. A second summand is upper bounded by the differential entropy of a Gaussian random variable (see Theorem 9.7.1 of [8]),

$$H(Y|x) \leqslant \frac{1}{2}\ln 2\pi e\left[\mathrm{Var}(Y|x)+\frac{1}{12}\right] \tag{C6}$$

$$= \frac{1}{2}\ln 2\pi e\left[x+\varepsilon_n(1+\varepsilon_n)+\frac{1}{12}\right]. \tag{C7}$$

The desired expression follows from carrying out the integration and using the definition of the incomplete gamma function.

[1] J. P. Gordon, Proc. IRE **50**, 1898 (1962).
[2] J. P. Gordon, in *Proceedings of the International School of Physics "Enrico Fermi," Course XXXI* (Academic Press, London, 1964), pp. 156–181.
[3] C. W. Helstrom, *Quantum Detection and Estimation Theory* (Academic Press, New York, 1976).
[4] A. S. Holevo, M. Sohma, and O. Hirota, Phys. Rev. A **59**, 1820 (1999).
[5] A. S. Holevo and R. F. Werner, Phys. Rev. A **63**, 032312 (2001).
[6] V. Giovannetti, S. Guha, S. Lloyd, L. Maccone, J. H. Shapiro, and H. P. Yuen, Phys. Rev. Lett. **92**, 027902 (2004).
[7] V. Giovannetti, S. Guha, S. Lloyd, L. Maccone, J. H. Shapiro, and B. J. Yen, Quantum Inf. Comput. **4**, 489 (2004).
[8] T. M. Cover and J. A. Thomas, *Elements of Information Theory*, Wiley Series in Telecommunications (Wiley, New York, 1991).
[9] C. M. Caves and P. D. Drummond, Rev. Mod. Phys. **66**, 481 (1994).
[10] S. D. Bartlett, T. Rudolph, and R. W. Spekkens, Rev. Mod. Phys. **79**, 555 (2007).
[11] M. A. Nielsen and I. L. Chuang, *Quantum Computation and Quantum Information* (Cambridge University Press, Cambridge, UK, 2000).
[12] R. A. Campos, B. E. A. Saleh, and M. C. Teich, Phys. Rev. A **40**, 1371 (1989).
[13] S. Karp, E. L. O'Neill, and R. M. Gagliardi, Proc. IEEE **58**, 1611 (1970).
[14] S. Verdú, Probl. Peredachi Inf. **32**, 86 (1996).
[15] A. Martinez, J. Opt. Soc. Am. B **24**, 739 (2007).
[16] M. Katz and S. Shamai (Shitz), IEEE Trans. Inf. Theory **50**, 2257 (2004).
[17] A. Lapidoth, in *Proceedings of the IEEE Inf. Theory Workshop, Bangalore, India* (IEEE, New York, 2002), pp. 1–4.
[18] W. H. Zurek, Phys. Today **44**, 36 (1991); e-print arXiv:quant-ph/0306072.